ADVANCED THEORY AND SIMULATIONS
www.advtheorysimul.com

Methane Adsorption Properties of Mn-Modified Graphene: A First-Principles Study

Yingjie Zhao, Yuhong Chen, Mingxia Song, Xiaocong Liu, Wenhui Xu, Meiling Zhang, and Cairong Zhang*

Graphene (GR), as a 2D carbon nanomaterial with high specific surface area, is one of the primary candidates for energy-storage applications. In this work, the adsorption properties of graphene and Mn-modified graphene (Mn-GR) systems for CH_4 molecules are investigated, based on first-principles density functional theory. It is found that intrinsic graphene adsorbs CH_4 molecules weakly. The single side can adsorb up to 4 CH_4 molecules, and the average adsorption energy is −0.220 eV per CH_4. Mn atom modification can significantly improve the adsorption performance of GR system on CH_4. The structure with the largest methane storage capacity is that the GR modified by two Mn atoms that are located in the spacer holes on the opposite sides. The system can adsorb 10 CH_4 molecules on both sides, the CH_4 adsorption amount can reach 32.93 wt%, and the average adsorption energy is −0.402 eV per CH_4. The interaction between the Mn atom and graphene is mainly between the d orbital of the Mn atom and the p orbital of the C atom. After the CH_4 molecule is adsorbed, charge transfer occurs between Mn atoms and CH_4, which results in a Coulomb attraction and enhances the adsorption performance of CH_4 molecules.

1. Introduction

The developments in science and technology have led to an increasing demand for energy. Fossil fuels are the main source of energy worldwide; however, their usage result in a production of a large amounts of harmful gases during the process of combustion, which cause environmental pollution and greenhouse effect.[1] Natural gas constitutes a major proportion of fossil fuels. Its main component is methane (CH_4).[2] Although it is not a renewable fuel, it has become a potential transitional fuel for future low-carbon energy.[3] CH_4 is also one of the reasons for the increasing greenhouse effect of the Earth's surface, accounting for ≈20% of global warming.[4] Therefore, the adsorption and storage of CH_4 is of great significance for the development and utilization of energy as well as environmental protection.

Traditionally, CH_4 is typically stored as compressed[5] or liquefied[6] natural gas, and natural gas adsorption technology (ANG)[7] is a new CH_4 storage method that can replace these conventional methods. Menon et al.[8] reviewed the adsorption properties and application prospects of several different types of traditional porous materials and reported that the adsorption capacity and surface area of silica gel, molecular sieve, and MCM-41 exhibit an evident linear relationship. Karl et al.[9] found that a high-porosity boron–nitrogen polymer (BLPs) had a maximum CH_4 uptake of 18.1 $cm^3\ g^{-1}$ at 273 K. Currently, most of the commonly used CH_4 adsorbents are MOF materials. Liu et al.[10] found that the surface area, pore size and pore volume of MOF and covalent organic framework (COF) porous materials have an important influence on the gas storage capacity of CH_4, and pointed out that the amount of adsorbed CH_4 by DUT-49 MOF material can reach up to 24.0 wt%. Spanopouls et al.[11] reported that the weight density and bulk density of CH_4 adsorbed by Cu-modified tbo-MOF under standard conditions can reach 26.6 wt% and 221 $cm^3\ cm^{-3}$, respectively. Zhao et al.[12] reported that a fluorine-containing zirconium-based MOF has a CH_4 content of 16.043 wt% at 298 K and 65 bar.

Graphene (GR) is a 2D carbon nanomaterial composed of a single atomic thickness composed of sp^2 hybrid orbitals.[13] In 2004, Novoselov et al.[14] of the University of Manchester first prepared a single layer of 2D graphene by mechanical stripping. This discovery stimulated scientists' interest in 2D materials. Graphene has been favored in many fields for its stable structure,[15] good chemical stability and electrical stability,[16] and high specific surface area.[17] For example, graphene exhibits high sensitivity and adsorption characteristics for certain gases, and is used in gas detection.[18-20] It also exhibits good hydrogen storage performance, and researchers have reported that its modifications by metals and nonmetallic elements improve the hydrogen storage performance of the system.[21,22] Studies have shown that graphene is one of the potential mediators for

Y. Zhao, Prof. Y. Chen, M. Song, X. Liu, W. Xu, M. Zhang, Prof. C. Zhang
School of Science
Lanzhou University of Technology
Lanzhou 730050, China
E-mail: chenyh@lut.cn
Prof. Y. Chen, Prof. C. Zhang
State Key Laboratory of Advanced Processing and Recycling of Non-Ferrous Metals
University of Technology
Lanzhou 730050, China

The ORCID identification number(s) for the author(s) of this article can be found under https://doi.org/10.1002/adts.202000035

DOI: 10.1002/adts.202000035

the storage of CH_4,[23] but CH_4 has a lower adsorption energy on the intrinsic graphene surface. Yang et al.[24] found that the adsorption energy of CH_4 increased with an increase in the number of graphene layers, and the maximum adsorption energy was −0.267 eV. The surface activity and adsorption properties of graphene can be improved by using alkali metals,[22] alkaline earth metals[25] and transition metals[26-28] modification, or the introduction of B, N, and other atom doping.[29] Zhao et al.[30] reported that Al doping can increase the adsorption energy of CH_4; however, it deforms the structure. Using the Quantum-ESPRESSO software, Ghanbari et al.[31] calculated that the adsorption energy of CH_4 on Ag modified graphene surface was −0.166 eV, whereas that of CH_4 in aerobic environment was −0.399 eV, which was significantly higher than that of intrinsic graphene. Rad et al.[32] used the Gaussian software to calculate that the NH_3 and CH_4 gas molecules on Pt-modified graphene have higher adsorption energy, higher charge transfer, smaller intermolecular distance, and higher orbital hybridization than that of the original graphene, in which the adsorption energy of CH_4 increases to −0.485 eV. Chen et al.[33] studied that the adsorption energy of Li-modified carbon nanotubes adsorbing CH_4 is ≈−0.464 eV, which can be applied for the separation of nonhydrocarbons in biogas. Through a molecular dynamics simulation, Jiang et al.[34] obtained that the maximum adsorption capacity of 3D pillared carbon nanotube (CNT)–porous graphene (PG) nanowires to CH_4 was 44.7 wt% at 298 K and 40 bar. Liu et al.[35] used the VASP software to calculate that the adsorption energy of a single CH_4 molecule of a 2D TiB_4 monolayer film was −0.41 eV, and the storage amount reached 10.14 wt%. Hence, it can be concluded that the 2D material also has a good CH_4 storage performance compared to the MOF material.

The Advanced Research Projects Agency-Energy of the Department of Energy (DOE) proposes that the weight density of CH_4 adsorption on-board energy should be greater than 50 wt%.[36] At present, a majority of studies on the storage of CH_4 fail to meet this requirement. In this study, the adsorption performance of CH_4 on graphene and the effect of Mn modification on the adsorption performance of the graphene system were analyzed using the first-principles method. Based on this analysis, the adsorption amount of CH_4 was calculated. It is expected that this research can provide theoretical support for the manufacturing of new CH_4 storage materials.

2. Calculation Methods and Models

The calculation used in this study employs the CASTEP module under Material Studio 8.0 software,[37] based on the first-principles pseudopotential plane wave method considering density functional theory (DFT). A generalized gradient approximation (GGA)[38] under the Perdew–Burke–Ernzerhof (PBE) exchange correlation functional form is chosen, and the super soft pseudopotential is used to describe the interaction between electrons and ions. As the GGA functional may underestimate weak sorption energies, the van der Waals correction (i.e., DFT-D method) is used in the calculation.[39] All atoms in the calculation are completely relaxed. The convergence criterion of structural optimization is that the force of each atom is less than 0.01 eV $Å^{-1}$, the energy difference is less than 1.0×10^{-6} eV per atom, and the self-consistent field convergence threshold is 1.0×10^{-6} eV per atom. By testing the cutoff energy of the system and the sampling of the K-point considering calculation accuracy and calculation cost, the cutoff energy was considered as 400 eV, and the K-point sampling in the Brillouin zone is 5 × 5 × 1. This is basically consistent with the accuracy selected by Thierfelder et al.[40] during the calculation of graphene adsorption of methane. The calculation of the graphene unit cell satisfies the periodic boundary conditions, and the vacuum layer is set to 25 Å to avoid interlayer interactions.

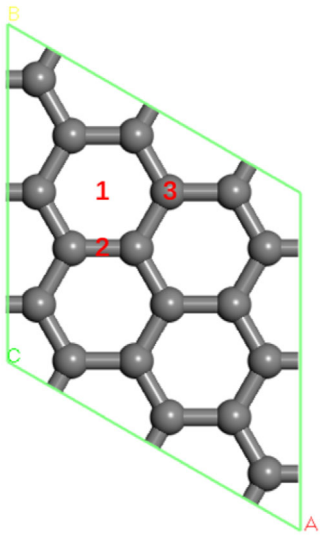

Figure 1. Geometric structure of graphene 3 × 3 supercells.

The binding energy (E_b) and average binding energy ($\bar{E}_b$) of the Mn atom on GR are defined as

$$E_b = E_{Mn+GR} - \left(E_{GR} + E_{Mn}\right) \quad (1)$$

$$\bar{E}_b = \left[E_{Mn+GR} - E_{GR} - nE_{Mn}\right] / n \quad (2)$$

where E_{Mn+GR}, E_{GR}, and E_{Mn} are the total energies of the Mn atom modified GR system (Mn-GR), GR system, and a free Mn atom, respectively. n represents the number of Mn atoms.

The adsorption energy (E_{ad}) and average adsorption energy ($\bar{E}_{ad}$) of the CH_4 molecule are defined as

$$E_{ad} = E_{iCH_4+Mn+GR} - E_{(i-1)CH_4+Mn+GR} - E_{CH_4} \quad (3)$$

$$\bar{E}_{ad} = \left[E_{iCH_4+Mn+GR} - E_{Mn+GR} - iE_{CH_4}\right] / i \quad (4)$$

where $E_{iCH_4+Mn+GR}$, $E_{(i-1)CH_4+Mn+GR}$, and E_{CH_4} are the total energies of the system with i and $i-1$ CH_4 molecules and one free CH_4 molecule, respectively.

The graphene structure is selected as a 3 × 3 supercell, and the optimized structure is shown in **Figure 1**. The calculated C—C bond length in GR is 1.437 Å, and the lattice constant is 7.470 Å, which is in good agreement with the experimental value of 7.380 Å.[41] This shows that the selected calculation accuracy and calculation method are appropriate, and the results of the calculation are reliable.

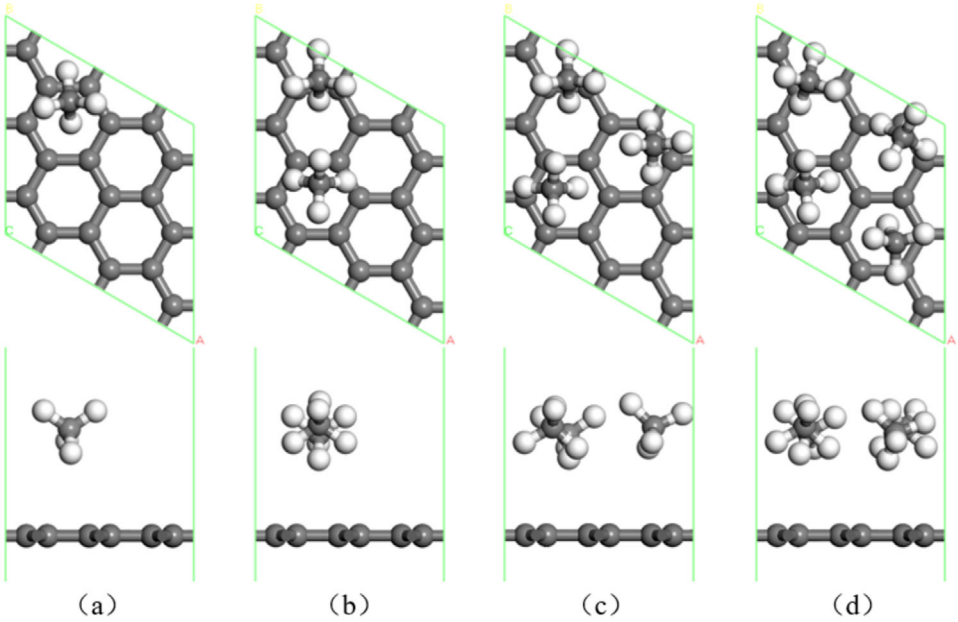

Figure 2. Geometry of intrinsic graphene adsorb 1–4 CH_4 molecules (gray and white spheres represent C and H atoms, respectively).

3. Results and Discussion

3.1. Adsorption of CH_4 on Intrinsic Graphene

First, the adsorption of CH_4 molecules on intrinsic graphene was studied. Consider the three different symmetrical positions, labeled 1, 2, and 3 in Figure 1, which represent the hole position of the C ring, the C–C bridge position, and the C top position, respectively. It was found that, at position 1, CH_4 molecules are most easily adsorbed on GR, and the adsorption energy is −0.359 eV, which is approximately the same as the optimal adsorption position of CH_4 obtained by Li et al.[42] Graphene 3 × 3 supercells can adsorb up to 4 CH_4 molecules on one side. The optimized geometry is shown in **Figure 2**a–d. The average adsorption energy of CH_4 molecules is found to be −0.227 eV per CH_4, and the adsorption energy is low.

3.2. Adsorption of CH_4 on Single Mn Atom Modified GR System

3.2.1. A Single Mn Atom Modifies the Geometry of GR

Due to the weak adsorption performance of intrinsic graphene on CH_4 molecules, this paper uses the first four cycles of alkali metal, alkaline earth metal, and transition metal modified graphene to perform CH_4 adsorption performance testing. The results show that the adsorption energy of CH_4 is greater when V, Fe, Mn, and Ni are modified (absolute value is greater than 0.6 eV), and the adsorption energy of CH_4 is between −0.2 and −0.4 eV when other metals are modified. However, when V, Fe, and Ni modified graphene adsorbs multiple methane molecules, the methane and the substrate deform or collapse. Mn is an important transition metal element, and its valence electron configuration is $3d^5 4s^2$, which indicates that it has some special physical and chemical properties. Lu et al.[43] found that the adsorption performance of Mn-modified graphyne on gas molecules is significantly improved, as compared to the original graphyne. Mn atom-modified graphene has a stable structure and significantly improves the adsorption energy of CH_4 molecules. Therefore, the modification of Mn atom is used for subsequent research.

First, the modification position of Mn on GR was studied. When a single Mn atom is modified, three different symmetrical positions are considered, which are positions 1, 2, and 3 in Figure 1. The calculation results show that when the Mn atoms are placed at positions 2 and 3, they are moved to the pore positions after optimization. Hence, the Mn atoms are most easily adsorbed on the GR at position 1. The optimized geometry is shown in **Figure 3**a. Mn atom is located in the pore position of the C ring, its binding energy is −3.282 eV, the distance between the Mn atom, and the GR plane is 1.494 Å.

According to the Mulliken charge population analysis, it was found that in the Mn-GR system, the charge transfer of Mn atoms to the graphene substrate was 1.16 e, and a strong electrostatic effect was generated between them. **Figure 4**. shows the partial state of the density (PDOS) of the Mn-GR system. It can be seen that in the range from −1.61 to 0.87 eV, the s and d orbitals of Mn atom have resonance peaks with the p orbitals of C atoms. That means that the s and d orbitals of Mn interact with the p orbital of C. However, compared with the s orbital of Mn atom, the d orbital of Mn atom and p orbital of C atom has stronger resonance peaks. Therefore, the valence band of Mn-GR system is mainly derived from the interaction between the p orbital of the C atom and the d orbital of the Mn atom.

3.2.2. Adsorption of CH_4 on Mn-GR System

The Mn-GR system can adsorb up to 4 CH_4 molecules on one side, and the optimized geometric structures are shown in **Figure 5**a–d. It is evident that the CH_4 molecule is mainly

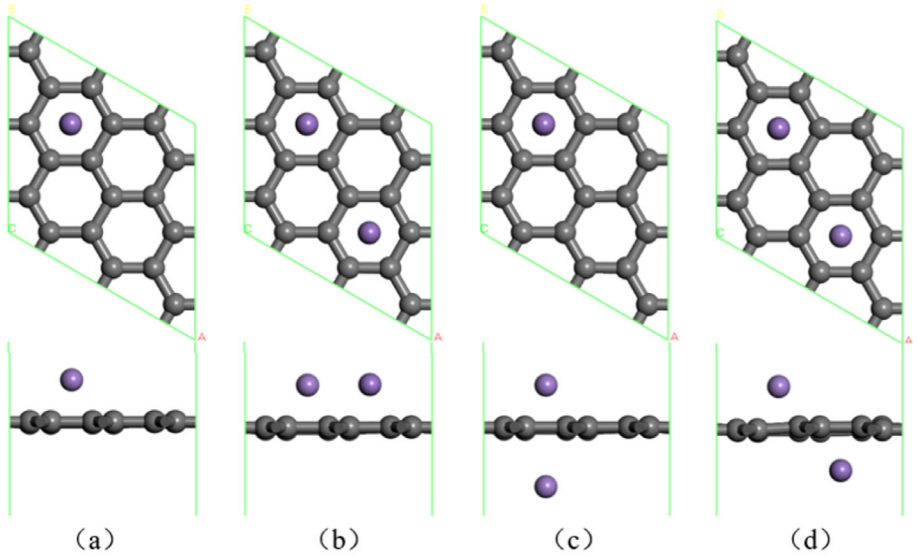

Figure 3. Geometric structure of Mn atom modified GR system: a) a single Mn atom modification; b–d) two Mn atom modification (purple ball represents Mn atom).

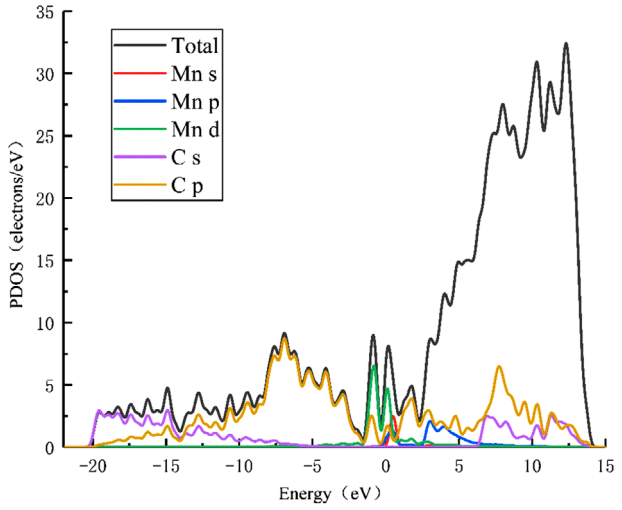

Figure 4. Partial state of the density (PDOS) of Mn-GR system.

adsorbed around the Mn atom. The adsorption energy of the first CH_4 molecule is −0.861 eV, which is significantly larger than the adsorption energy of the intrinsic graphene to the CH_4 molecule. It is also higher than that of the Ag modified[31] and Pt modified[32] graphene. Furthermore, the modification of GR by Mn atoms considerably improves the CH_4 adsorption capacity of the system.

Table 1 lists the adsorption energies (E_{ad}) and average adsorption energies ($\overline{E}_{ad}$) of the CH_4 molecule on the GR system and the Mn-GR system, the distance $d_{Mn\text{-}Gr}$ between the Mn atom and the GR plane, and the distance d_{Mn-CH_4} between the C atom and the Mn atom in each CH_4 molecule of the Mn-GR system. It can be seen that the adsorption energy of each CH_4 molecule on the GR system does not change significantly, and the overall change is small. The adsorption energy of CH_4 molecules on the Mn-GR system decreases as the number of CH_4 molecules increases. Additionally, the distance between Mn atoms increases, which indicates that Mn atoms play an important role during the CH_4 adsorption process. Due to the limitation of the adsorption space, the Mn-GR system can adsorb up to 4 CH_4 molecules on one side with an average adsorption energy of −0.510 eV per CH_4. Compared with the intrinsic graphene system, there is a significant improvement in the average adsorption energy of CH_4 molecules.

Based on the Mulliken charge layout before and after the adsorption of CH_4 molecules, the charge transfers and bonding between atoms can be analyzed. **Table 2** shows the Mulliken charge layout number before and after the adsorption of a CH_4 molecule in the Mn-GR system. Among them, C, H1, H2, H3, and H4 respectively represent the C atom and the 4 H atoms on the CH_4 molecule. H1 is located directly above the Mn atom, H2 is an H atom facing upward, and the H3 and H4 atoms are facing downward. It can be seen that the C atom in the CH_4 molecule is negatively charged and the four H atoms on the surface are all positively charged. Therefore, there is a significant repulsive force between the CH_4 molecules, making it difficult for multiple CH_4 molecules to aggregate at the same adsorption site. In a limited adsorption space, the GR system can only adsorb 4 CH_4 molecules on one side, and the adsorption energy is small. However, in the Mn-GR system, Mn atoms are positively charged, and the graphene substrate is negatively charged, which makes positively charged graphene and CH_4 molecules on the surface more susceptible to adsorption. After the CH_4 molecule was adsorbed on the Mn-GR system, H1, H3, and H4 received electrons to different degrees. Among them, H3 and H4 obtained 0.20 and 0.21 e, respectively. The positively charged surface area of the CH_4 molecule decreased, and the intermolecular repulsion effect weakened. The CH_4 molecule as a whole gets electrons (0.38 e) negatively charged. The Mn atom loses electrons (0.39 e) and becomes more positively charged. After adsorption, the electrons are mainly transferred from Mn

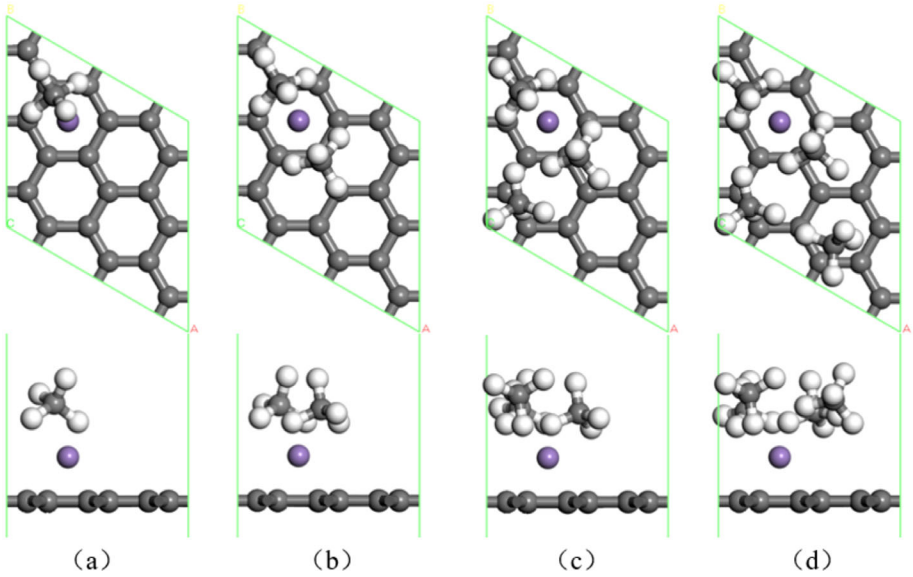

Figure 5. Geometric structure of 1–4 CH_4 molecules adsorbed by Mn-GR system.

Table 1. Energy and geometric parameters of CH_4 molecule in GR and Mn-GR systems.

	Number of CH_4	1	2	3	4
GR	E_{ad} [eV]	−0.359	−0.136	−0.194	−0.220
	$\bar{E}_{ad}$ [eV]	−0.359	−0.248	−0.230	−0.227
Mn-GR	E_{ad} [eV]	−0.861	−0.625	−0.303	−0.250
	$\bar{E}_{ad}$ [eV]	−0.861	−0.743	−0.597	−0.510
	d_{Mn-GR} [Å]	1.580	1.599	1.587	1.581
	d_{Mn-CH_4} [Å]	2.159	2.318	4.190	5.179

Table 2. The Mulliken layout number before and after the adsorption of a CH_4 molecule in the Mn-GR system.

	Before adsorption [e]				After adsorption [e]			
Atom	s	p	d	Charge	s	p	d	Charge
H1	0.73			0.27	0.76			0.24
H2	0.73			0.27	0.71			0.29
H3	0.73			0.27	0.93			0.07
H4	0.73			0.27	0.94			0.06
C	1.51	3.59		−1.10	1.43	3.63		−1.06
Mn	−0.10	−0.25	6.19	1.16	−0.03	−0.07	6.18	1.55

atoms to CH_4 molecules. Positively charged Mn atoms and negatively charged CH_4 molecules produce a Coulomb attraction, which improves the adsorption energy of the CH_4 molecules.

According to the charge difference density diagram, the charge transfers of the system before and after the adsorption of CH_4 molecules can be observed more intuitively. **Figure 6** shows the charge differential density of a CH_4 molecule adsorbed by the Mn-GR system. The blue and yellow isosurfaces represent the electron gain and electron loss regions, respectively. It can be seen that the charge transfer is mainly distributed between Mn atoms, and H3, H4, and C atoms also have a small amount of charge transfer. Generally, Mn atoms and CH_4 molecules undergo charge transfer, which results in Coulomb interaction and enhances the adsorption performance of CH_4 molecules, which is consistent with Mulliken charge analysis results.

To further study the interaction between Mn atoms and adsorbed CH_4 molecules, the PDOS of CH_4 molecules and Mn atoms after adsorption was analyzed (as shown in **Figure 7**). It can be seen that the 1s orbital of the H atom and the 3d orbital of the Mn atom overlap around −8.0 and −15.0 eV, which indicates that the main interaction occurs between these orbitals; this is in accordance with the Mulliken charge layout analysis of the main charge transfer. The DOS peak of the H atom of the second CH_4 molecule at −16.0 to −6.0 eV is lower than that of the first CH_4 molecule, indicating that the interaction between the second CH_4 molecule and the Mn atom is slightly weakened. This explains that the adsorption energy of the second CH_4 molecule is less than that of the first. With an increase in the number of adsorbed CH_4 molecules, the DOS peak of CH_4 molecules decreases and moves toward deeper energy levels, which indicates that the interaction between CH_4 molecule and Mn atom is gradually weakened; this is consistent with the gradual decrease of the adsorption energy when the Mn-GR system adsorbs CH_4 molecules. In addition, with the increase of the number of adsorbed CH_4 molecules, the distance between CH_4 molecules and Mn atoms also increases, indicating the interaction decreases.

3.3. Adsorption of CH_4 on two Mn-Atom-Modified GR Systems

3.3.1. Geometric Structure of GR Modified by Two Mn Atoms

In the case where GR is modified by two Mn atoms, three stable structures are calculated, as shown in Figure 3b–d. Figure 3b

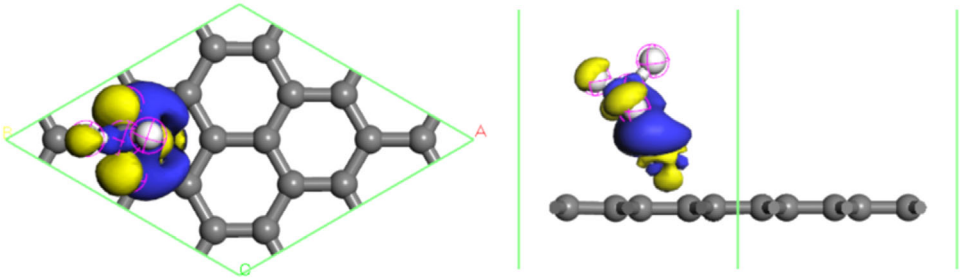

Figure 6. Charge difference density diagram of a CH_4 molecule adsorbed by Mn-GR system.

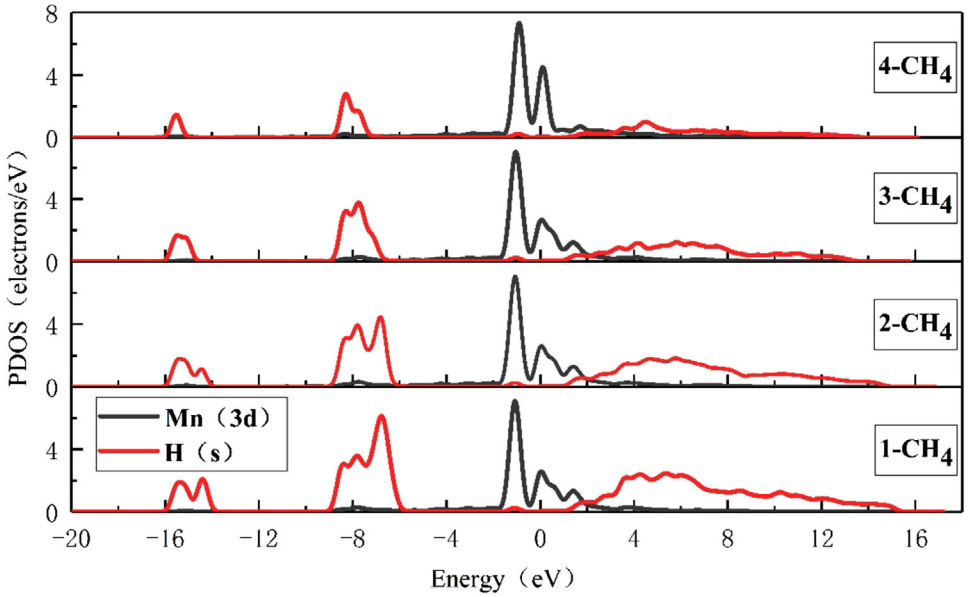

Figure 7. PDOS of 1–4 CH_4 molecules adsorbed on Mn-GR system.

shows that two modified Mn atoms are located on the same side of GR, and the adsorption space is limited. Hence, it is difficult to increase the amount of adsorbed CH_4 molecules. Each Mn-modified atom is an active adsorption site. Double-sided modification can greatly significantly increase the storage space of CH_4 molecules, thereby increasing the amount of CH_4 molecules adsorbed. The average binding energy of the Mn atoms shown in Figure 3c is −2.662 eV, and the average binding energy of the Mn atoms shown in Figure 3d is −3.590 eV, which is equivalent to the structure shown in Figure 3b, and the structure is more stable. In addition, the cohesion energy of Mn is −2.920 eV,[44] which is less than the absolute value of the average binding energy of Mn atoms in the structure shown in Figure 3d. Thus, Mn atoms do not agglomerate easily. Therefore, the structure shown in Figure 3d was used to study the molecular properties of CH_4.

3.3.2. Methane Reserves of Two Mn Atom Modified GR Systems

The two Mn-modified GR systems can adsorb up to 5 CH_4 molecules on one side. The optimized geometric structures are shown in **Figure 8**a–e. It can be seen that when the fifth CH_4 molecule is adsorbed, the large distance between this molecule and the GR plane results in the phenomenon of layered adsorption. This is due to the limited adsorption space around the Mn atoms and the repulsion from the positively charged surface of the CH_4 molecule. The two Mn-modified GR systems can adsorb 10 CH_4 molecules on both sides, and the optimized geometry of the 6th to 10th CH_4 molecules on the second side is shown in Figure 8f–j. Compared with single-sided adsorption, this structure is more symmetrical. The average adsorption energy of the CH_4 molecules is −0.402 eV per CH_4, and the adsorption amount of CH_4 molecules is 32.93 wt%. This value is a significant improvement compared to the adsorption capacity of MOF materials,[11,12] which is closer to the standards proposed by the US DOE.[36]

Table 3 lists the adsorption energy (E_{ad}) and the average adsorption energy ($\bar{E}_{ad}$) of CH_4 molecules on the two Mn-modified GR systems, the distance (d_{GR-CH_4}) between the C atom of each CH_4 molecule and the GR plane, and the distance (d_{Mn-CH_4}) between the C atom of each CH_4 molecule and the Mn atom. It can be seen that the distance between the first and second CH_4 molecules adsorbed on each side and the Mn atom is relatively close, and the adsorption energy high. Due to the phenomenon of layered adsorption, the fifth CH_4 molecule is at a greater distance

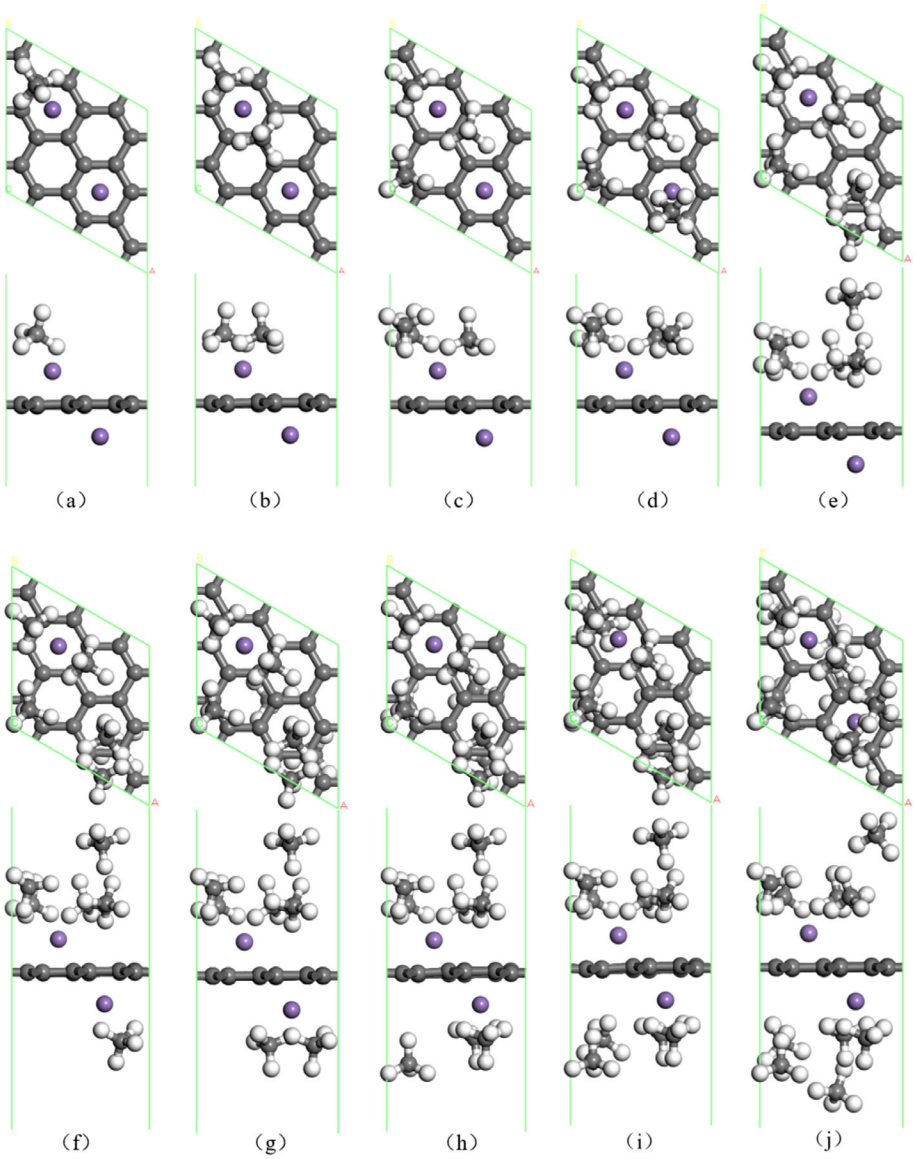

Figure 8. The most stable structure for adsorption of 1–10 CH_4 molecules by two Mn atom-modified GR systems.

Table 3. Energy parameters and geometric parameters of CH_4 molecule on two Mn-modified GR systems.

Number of CH_4	E_{ad} [eV]	$\bar{E}_{ad}$ [eV]	d_{GR-CH_4} [Å]	d_{Mn-CH_4} [Å]
1	−0.829	−0.829	3.105	2.253
2	−0.682	−0.755	3.098	2.275
3	−0.164	−0.558	3.775	4.157
4	−0.239	−0.479	3.165	5.179
5	−0.094	−0.402	5.947	6.156
6	−0.806	−0.469	3.213	2.251
7	−0.738	−0.507	3.071	2.266
8	−0.075	−0.453	4.860	4.499
9	−0.284	−0.435	3.472	5.679
10	−0.111	−0.402	5.692	6.201

from the Mn atom and its adsorption energy is low. The Mulliken charge layout and density of state analysis show that there is a strong charge transfer and orbital interaction between the CH_4 molecule and the Mn atom. Moreover, it is evident that the Mn atom plays an important role during the adsorption process of CH_4 molecules. When the distance between CH_4 molecules and Mn atom increases, the interaction weakens, leading to a decrease in adsorption performance. The lower adsorption energy of the 8–10 CH_4 molecules on the second side is also related to the distance from the Mn atom.

To eliminate the edge effects, a 2 × 2 cell expansion was performed on the basis of the 3 × 3 supercells of the graphene described above, to obtain a large unit cell, that is, a 6 × 6 supercell of graphene, for the CH_4 molecule adsorption test. The optimized geometry of the super-large unit cell adsorbing 40 CH_4 molecules, as shown in **Figure 9**, contains 112 C atoms,

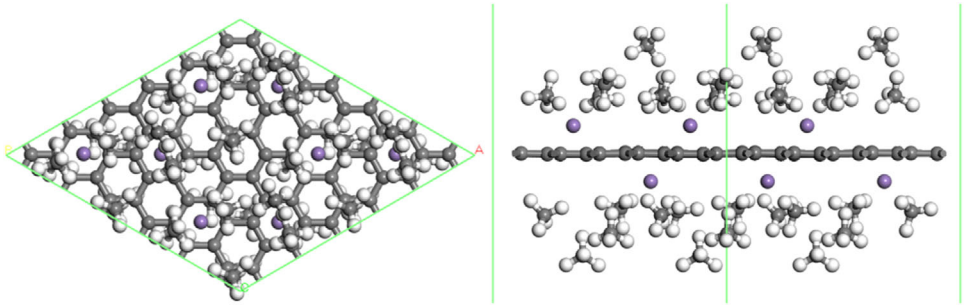

Figure 9. Geometrically optimized structure of Mn-GR super unit cell adsorption of CH_4 molecules.

160 H atoms, and 8 Mn atoms. The calculation results show that the average binding energy of Mn atoms in the system is −3.498 eV, without agglomeration, and the average adsorption energy of CH_4 molecules is −0.415 eV per CH_4, which is consistent with the results before cell expansion. This proves that the system is stable, and the results are reasonable.

4. Conclusion

Based on the first-principles density functional theory, the performance of graphene on CH_4 molecules was studied. The study found that intrinsic graphene has a weak adsorption of CH_4 molecules. The most stable adsorption position of a single CH_4 molecule is the graphene pore position, and the adsorption energy is −0.359 eV. One side can adsorb a maximum of 4 CH_4 molecules, with an average adsorption energy of −0.227 eV per CH_4. In the Mn-GR system, the most stable modification position of the Mn atom is at the center of the carbocyclic ring, and the binding energy is −3.228 eV. The modification of GR by Mn atom is shown to improve the CH_4 adsorption performance of the system. The Mn-GR system can adsorb 4 CH_4 molecules on one side, and the average adsorption energy is −0.510 eV per CH_4. The structure with the largest methane storage capacity is the GR modified by two Mn atoms, located at different pores on the opposite sides. This system can adsorb 10 CH_4 molecules on both sides, with an average adsorption energy of −0.402 eV per CH_4, and a storage capacity of CH_4 of 32.93 wt%. The adsorption of CH_4 molecules is mainly affected by Mn atoms, and the interaction between Mn atoms and graphene substrates is mainly the interaction between the d orbitals of the Mn atoms and the p orbitals of C atoms. The graphene substrate is negatively charged, and an electrostatic interaction with the positively charged CH_4 molecules on the surface exists. After the adsorption of CH_4 molecules, a charge transfer occurs between Mn atoms and CH_4 molecules. The CH_4 molecules are negatively charged, and the Mn atoms are positively charged. Hence, these produce a coulomb attraction and enhance the adsorption performance of the CH_4 molecules. In addition, the positive surface charge of the CH_4 molecule decreases after adsorption, and the intermolecular repulsion decreases, which is conducive to the improvement of adsorption capacity. Therefore, it can be concluded that the Mn-modified graphene system is one of the promising materials for methane storage applications.

Acknowledgements

The authors gratefully acknowledge the financial support from the National Natural Science Foundation of China (grant number 51562022), the Basic Scientific Research Foundation for Gansu Universities of China (grant number 05-0342), and the Special Program for Applied Research on Super Computation of the NSFC-Guangdong Joint Fund (second phase).

Conflict of Interest

The authors declare no conflict of interest.

Keywords

adsorption, CH_4, graphenes, Mn-modified materials

Received: February 21, 2020
Revised: March 27, 2020
Published online:

[1] D. Beerling, R. A. Berner, F. T. Mackenzie, M. B. Harfoot, J. A. Pyle, *Am. J. Sci.* **2009**, *309*, 97.
[2] K. Frank, J. T. G. Hamilton, B. Marc, R. C. J. N. Thomas, *Nature* **2006**, *439*, 187.
[3] T. A. Makal, J. R. Li, W. Lu, H. C. Zhou, *Chem. Soc. Rev.* **2012**, *41*, 7761.
[4] D. R. Feldman, W. D. Collins, S. C. Biraud, M. D. Risser, D. D. Turner, P. J. Gero, J. Tadić, D. Helmig, S. Xie, E. J. Mlawer, T. R Shippert, M. S. Torn, *Nat. Geosci.* **2018**, *11*, 238.
[5] M. Frick, K. W. Axhausen, G. Carle, A. Wokaun, *Transp. Res., D: Transp. Environ.* **2007**, *12*, 10.
[6] C. W. Remeljej, A. F. A. Hoadley, *Energy* **2006**, *31*, 2005.
[7] K. R. Matranga, A. L. Myers, E. D. Glandt, *Chem. Eng. Sci.* **1992**, *47*, 1569.
[8] V. C. Menon, S. J. Komarneni, *J. Porous Mater.* **1998**, *5*, 43.
[9] K. T. Jackson, M. G. Rabbani, T. E. Reich, H. M. El-Kaderi, *Polym. Chem.* **2011**, *2*, 2775.
[10] J. Liu, R. Zou, Y. Zhao, *Tetrahedron Lett.* **2016**, *57*, 4873.
[11] I. Spanopoulos, C. Tsangarakis, E. Klontzas, E. Tylianakis, G. Froudakis, K. Adil, Y. Belmabkhout, M. Eddaoudi, P. N. Trikalitis, *J. Am. Chem. Soc.* **2016**, *138*, 1568.
[12] D. Zhao, C. Yu, J. Jiang, X. Duan, L. Zhang, K. Jiang, G. Qian, *J. Solid State Chem.* **2019**, *277*, 139.
[13] R. H. Baughman, A. A. Zakhidov, W. A. De Heer, *Science* **2002**, *297*, 787.

[14] K. S. Novoselov, A. K. Geim, S. V. Morozov, D. Jiang, Y. Zhang, S. V. Dubonos, I. V. Grigorieva, A. A. Firsov, *Science* **2004**, *306*, 666.
[15] C. Lee, X. Wei, J. W. Kysar, J. Hone, *Science* **2008**, *321*, 385.
[16] N. M. R. Peres, *Vacuum* **2009**, *83*, 1248.
[17] H. K. Chae, D. Y. Siberio-Perez, J. Kim, Y. Go, M. Eddaoudi, A. J. Matzger, M. O'Keeffe, O. M. Yaghi, *Nature* **2004**, *427*, 523.
[18] X. Li, W. Cai, J. An, S. Kim, J. Nah, D. Yang, R. Piner, A. Velamakanni, I. Jung, E. Tutuc, S. K. Banerjee, L. Colombo, R. S. Ruoff, *Science* **2009**, *324*, 1312.
[19] F. Schedin, A. K. Geim, S. V. Morozov, E. W. Hill, P. Blake, M. I. Katsnelson, K. S. Novoselov, *Nat. Mater.* **2007**, *6*, 652.
[20] O. Leenaerts, B. Partoens, F. M. Peeters, *Phys. Rev. B* **2008**, *77*, 125416.
[21] M. Bartolomei, E. Carmona-Novillo, G. Giorgi, *Carbon* **2015**, *95*, 1076.
[22] B. Xu, X. L. Lei, G. Liu, M. S. Wu, C. Y. Ouyang, *Int. J. Hydrogen Energy* **2014**, *39*, 17104.
[23] X.-P. Chen, N. Yang, J. -M. Ni, M. Cai, H. -Y. Ye, C. K. Y. Wong, S. Y. Y. Leung, T.-L. Ren, *IEEE Electron Device Lett.* **2015**, *36*, 1366.
[24] D. Yang, N. Yang, J. Ni, J. Xiao, J. Jiang, Q. Liang, T. Ren, X. Chen, *Mater. Des.* **2017**, *119*, 397.
[25] G. Kim, S. H. Jhi, *J. Phys. Chem. C* **2009**, *113*, 20499.
[26] M. D. Ganji, H. Mazaheri, A. Khosravi, *Commun. Theor. Phys.* **2015**, *64*, 576.
[27] M. Gautam, A. H. Jayatissa, *Solid-State Electron.* **2012**, *78*, 159.
[28] M. Zhou, Y.-H. Lu, Y. -Q. Cai, C. Zhang, Y.-P. Feng, *Nanotechnology* **2011**, *22*, 385502.
[29] J. Dai, J. Yuan, P. Giannozzi, *Appl. Phys. Lett.* **2009**, *95*, 232105.
[30] W. Zhao, Q. Y. Meng, *Adv. Mater. Res.* **2012**, *602–604*, 870.
[31] R. Ghanbari, R. Safaiee, M. M. Golshan, *Appl. Surf. Sci.* **2018**, *457*, 303.
[32] A. S. Rad, H. Pazoki, S. Mohseni, D. Zareyee, M. Peyravi, *Mater. Chem. Phys.* **2016**, *182*, 32.
[33] J. -J. Chen, W. -W. Li, X. -L. Li, H. -Q. Yu, *Environ. Sci. Technol.* **2012**, *46*, 10341.
[34] H. Jiang, X. L. Cheng, *J. Mol. Graphics Modell.* **2018**, *85*, 223.
[35] Z. Liu, E. Wu, J. Li, S. Liu, *Phys. Chem. Chem. Phys.* **2019**, *21*, 13151.
[36] The Advanced Research Projects Agency – Energy (ARPA-E) of the U.S Department of Energy, DE-FOA-0000672: Methane Opportunities for Vehicular Energy (MOVE). https://arpa-e-foa.energy.gov/Default.aspx?Search=move&SearchType= (accessed: February 2020).
[37] M. D. Segall, P. J. D. Lindan, M. J. Probert, C. J. Pickard, P. J. Hasnip, S. J. Clark, M. C. Payne, *J. Phys.: Condens. Matter* **2002**, *14*, 2717.
[38] J. P. Perdew, K. Burke, M. Ernzerhof, *Phys. Rev. Lett.* **1996**, *77*, 3865.
[39] T. Björkman, A. Gulans, A. V. Krasheninnikov, R. M. Nieminen, *Phys. Rev. Lett.* **2012**, *108*, 235502.
[40] C. Thierfelder, M. Witte, S. Blankenburg, E. Rauls, W. G. Schmidt, *Surf. Sci.* **2011**, *605*, 746.
[41] K. T. Chan, J. B. Neaton, M. L. Cohen, *Phys. Rev. B* **2008**, *77*, 235430.
[42] K. Li, H. Li, N. Yan, T. Wang, Z. Zhao, *Appl. Surf. Sci.* **2018**, *459*, 693.
[43] Z. Lu, P. Lv, D. Ma, X. Yang, S. Li, Z. Yang, *J. Phys. D: Appl. Phys.* **2018**, *51*, 065109.
[44] K. Charles, R. W. Hellwarth, *Phys. Today* **1957**,*10*, 43.